



LUND UNIVERSITY

Intensity dependent photon echo relaxation in rare earth doped crystals

Kröll, Stefan; Xu, E.; Kim, M. K.; Mitsunaga, M.; Kachru, R.

Published in:
Physical Review B (Condensed Matter)

DOI:
[10.1103/PhysRevB.41.11568](https://doi.org/10.1103/PhysRevB.41.11568)

1990

[Link to publication](#)

Citation for published version (APA):
Kröll, S., Xu, E., Kim, M. K., Mitsunaga, M., & Kachru, R. (1990). Intensity dependent photon echo relaxation in rare earth doped crystals. *Physical Review B (Condensed Matter)*, 41(16), 11568-11571.
<https://doi.org/10.1103/PhysRevB.41.11568>

Total number of authors:
5

General rights

Unless other specific re-use rights are stated the following general rights apply:
Copyright and moral rights for the publications made accessible in the public portal are retained by the authors and/or other copyright owners and it is a condition of accessing publications that users recognise and abide by the legal requirements associated with these rights.

- Users may download and print one copy of any publication from the public portal for the purpose of private study or research.
- You may not further distribute the material or use it for any profit-making activity or commercial gain
- You may freely distribute the URL identifying the publication in the public portal

Read more about Creative commons licenses: <https://creativecommons.org/licenses/>

Take down policy

If you believe that this document breaches copyright please contact us providing details, and we will remove access to the work immediately and investigate your claim.

LUND UNIVERSITY

PO Box 117
221 00 Lund
+46 46-222 00 00

Intensity-dependent photon-echo relaxation in rare-earth-doped crystals

S. Kröll,* E. Y. Xu, and M. K. Kim†

Molecular Physics Laboratory, SRI International, Menlo Park, California 94025

M. Mitsunaga

NTT Basic Research Laboratories, Musashino-shi, Tokyo 180, Japan

R. Kachru

Molecular Physics Laboratory, SRI International, Menlo Park, California 94025

(Received 12 January 1990)

Photon-echo-relaxation measurements made on the $^3\text{H}_4\text{-}^3\text{P}_0$ transition of 0.01 at. % Pr^{3+} :YAG (where YAG represents yttrium aluminum garnet), $^3\text{H}_4\text{-}^1\text{D}_2$ transition in 0.1 at. % Pr^{3+} : YAlO_3 , and $^7\text{F}_0\text{-}^5\text{D}_0$ transition in 0.25 at. % Eu^{3+} : YAlO_3 show that the photon-echo relaxation rate increases when the intensities of the excitation pulses are increased. Although a part of the relaxation-rate increase in Pr^{3+} :YAG may be attributed to an instantaneous spectral diffusion (ISD) in which the presence of excited neighboring Pr^{3+} ions change the local field and the absorption frequency of the rare-earth ions, our data deviate significantly from the ISD-model predictions. An additional intensity-dependent relaxation mechanism is required to explain the results.

The rare-earth-doped crystals are not only good laser materials, but also exhibit extremely narrow homogeneous linewidths at liquid-helium temperatures.¹⁻⁵ The two-pulse photon echo is an excellent technique to measure the dephasing time because its decay does not depend on the inhomogeneous strain broadening. Taylor and Hessler⁶ have predicted that the instantaneous spectral diffusion (ISD) would cause the photon-echo relaxation rate to depend on the intensities of the excitation pulse used to create the photon echo. However, a previous experiment in ruby⁷ failed to detect any intensity dependence but later Liu *et al.*⁸ reported intensity dependent frequency shifts. In the ISD model, the change in the electric dipole moment of the excited ion causes a shift in the local electric field at the site of a neighboring ion. The ISD interaction is essentially static (i.e., it is produced by an interaction whose time scale is large compared with the time scales of our experiment) even though it manifests itself in the photon echo as an homogeneous relaxation.

In this Brief Report, we report the observation of a strong increase of the photon-echo relaxation rate with the intensity of the excitation pulse in Pr^{3+} :YAG (where YAG represents yttrium aluminum garnet), Pr^{3+} : YAlO_3 , and Eu^{3+} : YAlO_3 . Recently, Huang *et al.*⁹ have also observed intensity-dependent photon-echo relaxation rates in Eu^{3+} : Y_2O_3 and they interpreted their results in terms of ISD. Our measurements indicate that additional processes may be needed to describe the intensity dependence of the photon-echo relaxation on the $^3\text{H}_4\text{-}^3\text{P}_0$ transition in Pr^{3+} :YAG. We suggest that a part of the observed increase is due to the static broadening and the concomitant intensity-dependent frequency shift⁹ caused by instantaneous spectral diffusion, and that an additional (as yet unidentified) mechanism is also required to explain our results. The result we have obtained has significance for all photon-echo work in solids, particularly those done with

pulsed-dye lasers.

If a two-level system is reasonably excited by two laser pulses, which are short compared to T_2 , at times $t=0$ and $t=\tau$, the photon-echo intensity I_e emitted at time $t=2\tau$ is expressed as

$$I_e(\tau) = I_e(0)e^{-4\tau/T_2}, \quad (1)$$

In Eq. (1) it is usually assumed that the parameter T_2 , also referred to as the homogeneous or dephasing time, is a constant for a given transition in a crystal. Below, we will show that T_2 depends on the intensity of the excitation pulses.

The experimental apparatus consists of a pair of Nd:YAG-pumped pulsed-dye lasers (PDL's) and a krypton-ion-laser-pumped ring-dye laser (RDL). In the Pr^{3+} :YAG measurements the two dye lasers are resonant with the $^3\text{H}_4\text{-}^3\text{P}_0$ absorption line ($\lambda=4870 \text{ \AA}$) that connects the lowest Stark components of the $^3\text{H}_4$ ground state and $^3\text{P}_0$ excited state of the 0.01 at. % Pr^{3+} :YAG crystal. The inhomogeneous width of the optical transition is determined from absorption measurements⁴ to be 2.0 cm^{-1} . The two independently triggerable Nd:YAG-pumped dye lasers each provide a single excitation pulse for the two-pulse photon-echo sequence while the pulse sequence from the RDL is provided by an acousto-optic modulator. The pulses produced by the PDL's have a 5-nsec length, a 0.5-cm^2 cross-sectional area, and a spectral linewidth of 1 or 10 GHz (with or without an intracavity étalon). The Pr :YAG crystal is immersed in a liquid-helium cryostat and the sample temperature was, for most of the measurements, fixed at 1.5 K. The photon echo is produced by combining the output of the two PDL's with a beam combiner and focusing the light beams inside the crystal with a 50-cm focal-length lens.

The top (bottom) trace in Fig. 1 labeled RDL, RDL (PDL,PDL) shows the typical semilog plot of echo inten-

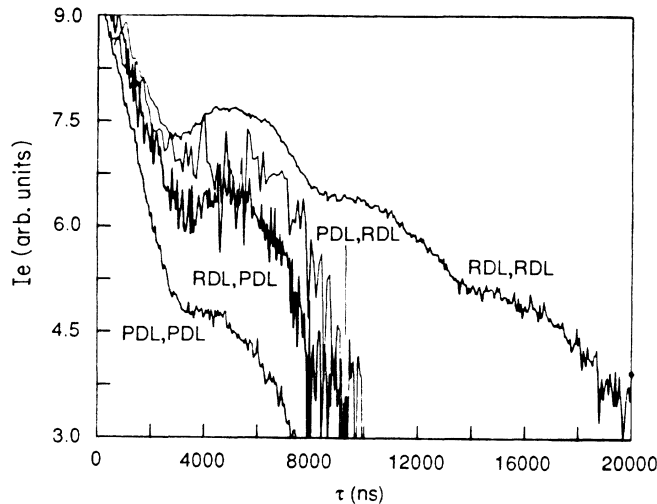


FIG. 1. Photon-echo intensity decay as a function of excitation-pulse separation. The first and second excitation pulses are produced from (a) PDL; (b) PDL and RDL, respectively; (c) RDL and PDL, respectively; and (d) RDL.

sity as a function of RDL (PDL) excitation-pulse separation in steps of 50 nsec. In Fig. 1 we believe the modulation is due to the hyperfine structure because our photon-echo measurement on the ${}^3\text{H}_4\text{-}{}^1\text{D}_2$ transition⁵ shows deeply modulated photon-echo intensity as a function of τ , with a modulation period corresponding to the inverse of the excited-state hyperfine splittings.⁵

Because the photon-echo decay is almost exponential, we use Eq. 1 to analyze our data and use T_2 as a parameter. The overall exponential decay time of the top (bottom) trace in Fig. 1 gives $T_2 = 16.5 \mu\text{s}$ ($4.5 \mu\text{s}$). What is surprising is that the measured dephasing time with the RDL is $\sim 350\%$ longer than that measured using the PDL. The trace labeled PDL,RDL in Fig. 1 shows the photon-echo relaxation when the first excitation pulse is a $10\text{-}\mu\text{J}$ 1-GHz spectrally wide PDL pulse and the second pulse is a 100-ns -long pulse from a 40-mW -average-power ring-dye laser. The T_2 parameter for this trace is $14.6 \mu\text{s}$. Figure 1 also shows the $T_2 = 9.1\text{-}\mu\text{s}$ relaxation of the photon-echo trace labeled RDL,PDL in which the RDL and the PDL provide the first and second excitation pulses, respectively. Below, we show that the excitation-pulse-intensity-dependent photon-echo decay accounts for the different echo-decay rates observed with the PDL and the RDL.

To determine the intensity-dependent photon-echo relaxation time, we have made extensive measurements of the echo decay as a function of excitation-pulse separation τ , similar to that shown in Fig. 1 with the PDL. The energy in each PDL excitation pulse is independently varied by inserting neutral-density filters and is measured by a calibrated energy meter (Molelectron J3-09). Figure 2 shows the variation of the measured T_2 versus the sum of the energies of the first and second excitation pulses produced by the PDL on a semilog scale. In the measurements in Fig. 2, the pulse energies of the two excitation pulses were equal. In another set of measurements, which we discuss below, the energy of one excitation pulse was

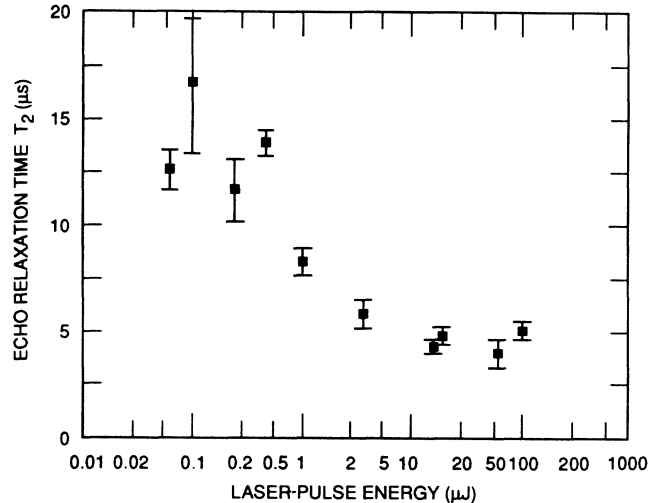


FIG. 2. Photon-echo relaxation time T_2 (inferred from the photon-echo decay as a function of pulse separation) plotted vs the sum of the energies in the two excitation pulses. Error bars are 1 standard deviation.

kept fixed, while the energy of the other excitation pulse was varied.

The data shown in Fig. 2 clearly show the large change in the value of the relaxation parameter T_2 as the energies of the excitation pulses are varied from $0.03 \mu\text{J}/\text{pulse}$ ($0.06\text{-}\mu\text{J}$ total energy) to $50 \mu\text{J}/\text{pulse}$. Specifically, when the input-pulse energies are reduced to $0.03 \mu\text{J}/\text{pulse}$, Fig. 2 shows a 3.5-fold increase in T_2 , compared to the echo produced with input pulses with $10 \mu\text{J}/\text{pulse}$. Furthermore, the $16.5\text{-}\mu\text{s}$ -long T_2 obtained at the lowest excitation-pulse energies (obtained from the PDL) is equal to $T_2 = 16.5 \mu\text{s}$ obtained from the photon-echo measurements made with the RDL.

We have also observed the intensity-dependent photon-echo relaxation on the ${}^3\text{H}_4\text{-}{}^1\text{D}_2$ transition in the 0.1 at. % $\text{Pr}^{3+}:\text{YAlO}_3$ and the ${}^7\text{F}_0\text{-}{}^5\text{D}_0$ transition in 0.25 at. % $\text{Eu}^{3+}:\text{YAlO}_3$ crystal using the PDL to produce the excitation pulses. Specifically, in $\text{Pr}^{3+}:\text{YAlO}_3$ we observe a $T_2 = 32 \mu\text{s}$ when the first and second pulses have energies of 0.75 and $1.0 \mu\text{J}$ per pulse, respectively. When the energies in the first and second excitation pulses are increased to 25 and $33 \mu\text{J}/\text{pulse}$, respectively, the relaxation time T_2 is reduced to $3.2 \mu\text{s}$. In $\text{Eu}^{3+}:\text{YAlO}_3$, we obtain an exponential decay with $T_2 = 53 \mu\text{s}$ when the excitation pulses are weak ($5 \mu\text{J}/\text{pulse}$). However, when the excitation pulses are strong ($80 \mu\text{J}/\text{pulse}$), we obtain a highly nonexponential decay and therefore the concept of T_2 becomes meaningless.¹⁰ Therefore, it may be assumed that the intensity-dependent effects we observe are quite general. We discuss below the physical mechanisms that may account for the intensity-dependent photon-echo decay in $\text{Pr}^{3+}:\text{YAG}$.

Taylor and Hessler have previously suggested that the instantaneous-spectral-diffusion (ISD) mechanism would result in an intensity-dependent photon-echo relaxation.⁶ The effect of ISD may be best understood by focusing our attention on a single rare-earth ion, labeled a , with absorption frequency ω_a , which participates in the echo for-

mation. The first excitation pulse produces a dipole moment p_a by creating a coherent superposition of the ground and excited electronic states. The presence of neighboring excited rare-earth ions causes a change in the local electrostatic field at the site of ion a . The change in the local field in turn results in the frequency shift $\Delta\omega$ of the ion absorption frequency. After the passage of the first excitation pulse, the rare-earth-ion dipole moment oscillates at a frequency $\omega_a + \Delta\omega_a$ and, therefore, the dipole acquires a phase

$$\phi_{a1} = \int_0^\tau [\omega_a(t') + \Delta\omega_a] dt'$$

prior to the excitation by the second excitation pulse. The second pulse not only changes the phase of the dipole moment p_a , but also the number density of excited rare-earth ions. This causes the absorption frequency of the ion to be changed to a new value, $\omega_a + \Delta\omega'_a(n')$, where n' is the change in the excited-state density after the second pulse. It can easily be shown that the phase of the dipole p_a at the echo time is given by¹¹

$$\phi_a(t=2\tau) = \left[\int_0^\tau \omega_a(t') dt' - \int_\tau^{2\tau} \omega_a(t') dt' \right] + \left[\int_0^\tau \Delta\omega_a dt' - \int_\tau^{2\tau} \Delta\omega_a(n') dt' \right]. \quad (2)$$

Since the echo amplitude is proportional to $\langle \exp i\phi_a(t=2\tau) \rangle$, where $\langle \dots \rangle$ indicates an ensemble average, the first term in Eq. (2) gives the homogeneous relaxation time T_2^0 due to the statistical variations of local fields at the echo atom site.¹² The second term in Eq. (2), which is due to quasistatic electric-dipole interaction,⁶ leads to an additional echo decay because of the incomplete rephasing of the dipole phase.

The intensity dependence of $\langle \exp i\phi_a(\tau=2\tau) \rangle$ arises through the parameter n' . To estimate the effect of the first-pulse intensity on n' , we note that the maximum time at which the echo is recorded is 10 μs . Assuming an excited-state radiative lifetime T_R of 50 μs [same as for the corresponding state in $\text{Pr}^{3+}:\text{LaF}_3$ (Ref. 13)], we note that a fraction $\exp(-\tau/T_R) \cong 0.9$ of the excited atoms still remain after 5 μs . Thus the change in n' for a strong first pulse is only 10% of the change that is obtained with a strong second pulse and consequently the ISD dependence on the first pulse is much weaker.

To compare the results shown in Fig. 2 with the ISD model, we have made measurements of the echo decay rate by varying the energy of the second (first) pulse while keeping the energy in the first (second) excitation pulse fixed at 0.08 μJ . These measurements are shown in Fig. 3. In Fig. 3, the open (solid) squares show the percent increase of the echo decay rate in percentage of unperturbed decay rate $1/T_2$ ($T_2 = 16.5 \mu\text{s}$) as the energy of the first (second) excitation pulse is increased from 0.15 to 33 μJ . In accordance with the ISD model discussed above, Fig. 3 shows a strong increase in the echo decay rate as the intensity of either of the pulses are increased.

We analyze our data in terms of the ISD model by assuming a Lorentzian kernel for the excitation-induced frequency shift, which is centered at zero-shifted frequency.⁹ If the first pulse is weak then by using Eq. (2) and the fact that the echo amplitude E is proportional to

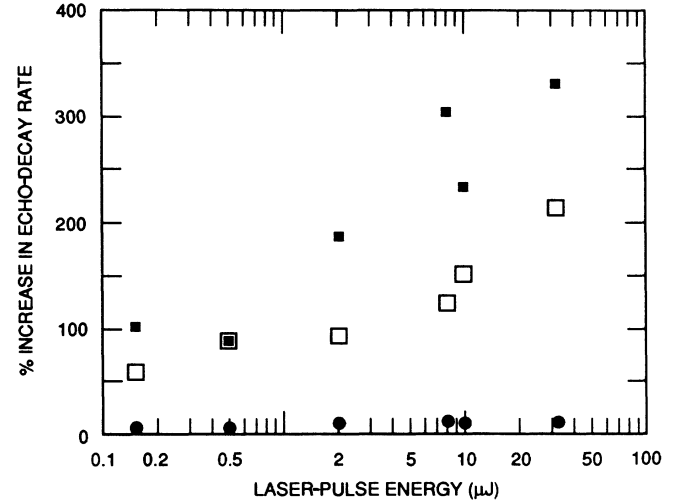


FIG. 3. The open (solid) squares show the increase of the echo-decay rate in percent of the unperturbed rate $1/T_2$ ($T_2 = 16.5 \mu\text{s}$) (see Fig. 2), as the energy of the first (second) excitation pulse is increased from 0.15 to 33 μJ . The solid circles show the fit to ISD model (see text).

$\langle \exp[-i\phi_a(t=2\tau)] \rangle$, we obtain $I_e \propto \exp\{-\tau[(4/T_2^0) + \gamma]\}$, where T_2^0 is the intensity-independent homogeneous relaxation time (16.5 μs) and γ the full width at half maximum (FWHM) of the Lorentzian kernel. Similarly for the case when the second pulse is weak, we obtain a nonsimple exponential decay given by $\exp\{-\tau[(4/T_2^0) + (\gamma\tau/T_R)]\}$ when $\tau/T_R \ll 1$. In our experiment the maximum value of τ is typically 5 μs , therefore the approximation $\tau/T_R \ll 1$ is a good one.

When we apply this model to our data shown in Fig. 3 we find that there is a discrepancy between the observed data and the ISD predictions. By using the ISD model outlined above for the 8.8- μs -long T_2 observed when the first and second pulses are 0.08 and 0.50 μJ , respectively, we get $\gamma = 211$ KHz (angular frequency). Using this value of γ , the ISD model predicts that the average T_2 (which is the average of T_2 at $\tau=0$ and 5 μs) under our experimental conditions (first-pulse energy = 0.5 μJ) should be 15.8 μs instead of the observed value of 8.7 μs . The solid circles in Fig. 3 show the predictions of the ISD model for the decay of the photon echo when the second pulse is weak that are calculated by using the γ parameter obtained by fitting the photon-echo decay when the first pulse is weak.

We therefore suggest that although the ISD is probably responsible for a part of the intensity-dependent photon-echo relaxation observed in our experiments, an additional relaxation mechanism appears necessary to explain the dependence of the relaxation rate on the first pulse energy. If we assume an intensity-dependent relaxation rate Γ , which varies with the excitation-pulse energy, then its contribution to the echo-intensity decay in the linear-excitation (small-area pulses) regime is given by $\exp(-2\Gamma\tau) [\exp(-4\Gamma\tau)]$, when the first (second) excitation pulse is weak. When we fit our low-energy data in Figs. 2 and 3 to the ISD and the intensity-dependent relaxation parameter Γ , we obtain a better fit to the data

shown in Fig. 3 with $\Gamma/\gamma=0.4$. Unfortunately the statistical error in our data does not allow us to accurately characterize the dependence of Γ on the excitation-pulse intensity. However, from our data it appears that this second mechanism (a) tends to produce exponential decays, even for a strong first pulse and a weak second pulse and (b) does not have an asymmetrical dependence on the first and second excitation pulse (see Fig. 3) as is the case with ISD.

A possible additional mechanism for the intensity-dependent decay is quiresonant energy transfer between two excited rare-earth ions.¹⁴ This would then, in contrast to ISD, be a homogenous dephasing process.

In conclusion, we have observed the excitation-pulse intensity-dependent photon-echo relaxation in $\text{Pr}^{3+}:\text{YAG}$, $\text{Pr}^{3+}:\text{YAlO}_3$, and $\text{Eu}^{3+}:\text{YAlO}_3$ crystals. A part of the intensity-dependent echo relaxation in $\text{Pr}^{3+}:\text{YAG}$ is attributable to the instantaneous spectral diffusion while the remainder can be explained if we assume an intensity-dependent dephasing process.

This research is supported by Nippon Telegraph and Telephone Corporation. S.K. wishes to acknowledge partial support from the Swedish Board of Technical Development (STU).

*Permanent address: Department of Atomic Physics/Combustion Centre, Lund Institute of Technology, Box 118, S-221 00, Lund, Sweden.

†Present address: Department of Physics and Astronomy, Wayne State University, Detroit, MI 48202.

¹Y. C. Chen, K. P. Chiang, and S. R. Hartmann, *Phys. Rev. B* **21**, 40 (1980).

²S. C. Rand, A. R. G. DeVoe, and R. G. Brewer, *Phys. Rev. Lett.* **43**, 1868 (1979).

³R. M. Shelby and R. M. Macfarlane, *Phys. Rev. Lett.* **45**, 1098 (1980).

⁴R. M. Macfarlane and R. M. Shelby, in *Spectroscopy of Solids Containing Rare Earth Ions*, edited by A. A. Kaplyanskii and R. M. Macfarlane (North-Holland, Amsterdam, 1987).

⁵M. K. Kim and R. Kachru, *Phys. Rev. B* **40**, 2082 (1989).

⁶D. R. Taylor and J. P. Hessler, *Phys. Lett.* **50A**, 205 (1974).

⁷S. Meth and S. R. Hartmann, *Phys. Lett.* **58A**, 192 (1976).

⁸G. K. Liu, N. F. Joubert, R. L. Cone, and B. Jacquier, *J. Lumin.* **38**, 34 (1987).

⁹J. W. Huang, J. M. Zhang, A. Lazama, and T. W. Mossberg, *Phys. Rev. Lett.* **63**, 78 (1989).

¹⁰M. Mitsunaga, E. Y. Xu, S. Kröll, and R. Kachru (unpublished).

¹¹R. Kachru, T. W. Mossberg, and S. R. Hartmann, *J. Phys. B* **13**, L363 (1980).

¹²J. R. Klauder and P. W. Anderson, *Phys. Rev.* **125**, 912 (1962).

¹³M. J. Weber, *J. Chem. Phys.* **48**, 4774 (1968).

¹⁴W. M. Yen, in *Spectroscopy of Solids Containing Rare Earth Ions*, edited by A. A. Kaplyanskii and R. M. Macfarlane (North-Holland, Amsterdam, 1987).